Soft Matter

Accepted Manuscript

ROYAL SOCIETY OF CHEMISTRY

www.rsc.org/softmatter

Journal Name

COMMUNICATION

Enzymatically Triggered Rupture of Polymersomes

Woo-Sik Jang,[a] Seung Chul Park,[a] Ellen H. Reed,[a] Kevin P. Dooley,[b] Samuel F. Wheeler,[c] Daeyeon Lee,*[a] and Daniel A. Hammer*[a, d]

Received 00th January 20xx,
Accepted 00th January 20xx

DOI: 10.1039/x0xx00000x

www.rsc.org/

Polymersomes are robust vesicles made from amphiphilic block co-polymers. Large populations of uniform giant polymersomes with defined, entrapped species can be made by templating of double-emulsions using microfluidics. In the present study, a series of two enzymatic reactions, one inside and the other outside of a polymersome, were designed to give rise to induced rupture of polymersomes. We measured how the kinetics of rupture were affected by altering enzyme concentration. These results suggest that protocells with entrapped enzymes can be engineered to secrete entrapped materials on cue.

Polymersomes are synthetic bilayer vesicles generated by self assembly of amphiphilic diblock copolymers in an aqueous environment.[1, 2] Due to their mechanical stability,[1, 3, 4] capacity for additional functionalization, and lower permeability,[5] polymersomes offer significant advantages over other bilayer vesicle in encapsulating and transporting enzymes,[6, 7] proteins,[8, 9] drugs,[9-14] and biomedical imaging and diagnostics.[15-18] Furthermore, the interior compartment of polymersomes has been engineered to serve as a micro-environment for protein expression,[8] gene expression,[19] and enzymatic reaction.[6, 7, 20-23] Blending each of these functions into different compartments within polymersomes could potentially lead to the development of protocells that mimic the metabolism,[6] enzymatic activity,[6, 7, 20-22, 24] and communications of real cells.[6, 8, 21, 25]

One key activity of a biological cell is secretion. To enable the release of encapsulated materials, which is a critical step for drug/gene delivery as well as exchange of materials (i.e., communication) between polymersomes, one needs to introduce a mechanism into protocells to engineer their rupture. Osmotic shock, for example, can lead to catastrophic volume change of polymersomes and rupture of the vesicle membrane.[26, 27] Electric fields applied to membranes with nonuniform charge density is another demonstrated route for release from protocells.[9, 28, 29] Depending on polymer chemistry, changes in the pH of solution can lead to the dissociation or reassembly of polymersome membranes, resulting in the release of the encapsulated biological molecules.[9] Optical stimuli have been used to trigger the release of encapsulated materials[25, 30, 31]; for example, porphyrin-based near-infrared (NIR) sensitive polymersomes have been induced to release the encapsulated materials with NIR irradiation. Somatologically favorable enzymatic reactions also have been used to control the release of encapsulants from polymersomes.[14, 17, 18, 23] Although these strategies have successfully shown the disruption of polymersomes to trigger the release of encapsulants, few studies have demonstrated the ability to tailor the rate of rupture/release using an enzyme cascade which can be readily controlled by the concentration of substrate.

In the present study, we demonstrate the triggered rupture of polymersomes via a two step cascade of enzymatic reactions. We prepared the polymersome using a poly(ethylene oxide-b-butadiene) amphiphilic diblock copolymer. The molecular weights of poly(ethylene oxide) and poly(butadiene) domains are 1.3 and 2.5 kDa, respectively. The molecular weight and amphiphilicity of this diblock copolymer facilitate the formation of robust bilayer vesicles. The first enzymatic reaction, catalyzed by hydrogen glucose oxidase (GOx), generates hydrogen peroxide (H_2O_2) and D-glucono 1, 5 lacton from D-glucose. The second enzymatic reaction, catalyzed by catalase, generates oxygen radical from H_2O_2, leading to the triggered rupture of polymersomes. H_2O_2 is a known reactive oxygen species that is formed during mitochondrial metabolism.[32-34] Antioxidant enzymes, such as the ones used in this work, detoxify or regulate the excess amount of reactive oxygen species. Thus, these enzymatic reactions mimic the somatological self-regulation of toxic materials within the human body, making this approach potentially suitable for future *in vivo* applications. One of the critical steps in realizing such a scheme is the encapsulation of catalase in the polymersomes, which we achieve using a recently developed microfluidic double emulsion method. We investigate the importance of the two enzymatic reactions in triggering the rupture of polymersomes and demonstrate that the rupture of polymersomes could be tuned by varying the concentration of enzymes.

A schematic illustration of enzymatically triggered rupture of polymersomes we explore in this work is shown in Figure 1(a). The design of our experiments is based on the initial hypothesis that H_2O_2 generated from GOx catalysis of D-glucose will penetrate the polymersome membrane and interact with encapsulated catalase within the polymersome. Catalase will then catalyze a reaction that

[a] Department of Chemical and Biomolecular Engineering, The University of Pennsylvania, Philadelphia PA.
[b] Department of Chemical Engineering, Rowan Univeersity, Glassboro NJ.
[c] Harriton High School, Rosemont PA
[d] Department of Bioengineering, The University of Pennsylvania, Philadelphia PA.
Email: hammer@seas.upenn.edu and daeyeon@seas.upenn.edu
* Corresponding Authors.
Electronic Supplementary Information (ESI) available: See DOI: 10.1039/x0xx00000x

generates free oxygen and causes vesicle failure and release. Catalase-loaded polymersomes were prepared with microfluidic water-in-oil-in-water (W/O/W) double emulsions. Microfluidic double emulsion-templated polymersomes have some amount of residual solvent upon preparation. Our previous work has shown that it takes up to 2 weeks to completely evaporate the residual solvent.[3] Therefore, we waited two weeks to remove solvent before using vesicles. Catalase-loaded polymersomes are dispersed in 1 ml solution of 290 mOsm D-glucose in a custom-made glass chamber. Prior to each experiment, we adjust the osmolality of the lumen of polymersomes to 290 mOsm using 10X phosphate-buffered saline (PBS) to prevent any effect of a change in osmotic pressure on the behavior of polymersomes. Subsequently, 0.2 ml of GOx solution was added to the chamber. Three different GOx solutions were prepared: 0.2, 1, and 2 wt. %, which are 0.0077, 0.0384, and 0.0768 mM, respectively. The total volume of the solution and D-glucose concentration were 1.4 ml and 208.1 mM, respectively. In the second enzymatic reaction, catalase catalyzed the conversion of H_2O_2 to water and oxygen (O_2), which induced the rupture of polymersomes.

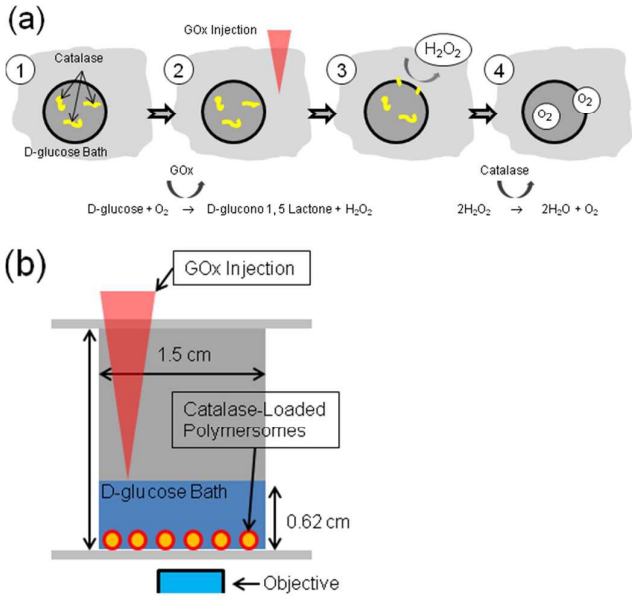

Figure 1. (a) Schematic illustration of the triggered rupture of polymersomes. (b) Custom-made glass bath for the observation of enzymatically triggered rupture of polymersomes. The dimension for glass bath was 1.5 × 1.5 × 2.0 cm^3 (width × length × height).

We studied the effect of GOx concentration on the dynamics of rupture of catalase-loaded polymersomes by monitoring the number of ruptured polymersomes as a function of time. To quantify the rupture rate of polymersomes, we define the surviving fraction (S_V) of polymersomes: $S_V(t)$ is defined as $N(t)/N_0$ where $N(t)$ is the number of intact polymersomes in the field of view (FOV) at time t and N_0 is the initial number of polymersomes in the FOV. Figure 2(a) shows the monitored rupture behavior for catalase-loaded polymersomes with three different GOx concentrations: 0.2, 1.0, and 2.0 wt. %. We determined the rupture of polymersomes at one minute intervals. For each GOx concentrations, we performed five experiments. The initial numbers of polymersomes were 73.4 ± 19.2, 90.6 ± 37.8, and 65.2 ± 11.9 for 0.2, 1, and 2 wt. % GOx concentrations, respectively. The onset and termination points for S_V are defined as: $S_V(t_{onset})$ = 90 % and $S_V(t_{termination})$ = 10 %. Figure 2(b) shows that the onset and termination times decrease with increasing GOx concentration. Figure 2(b) inset shows the active duration (d) for each GOx concentrations: $d = t_{Termination} - t_{Onset}$. From d, we can estimate the rupture rate of polymersomes under different GOx concentrations (Figure 2(c)). The rupture rate at 0.2 wt. % GOx is significantly smaller than that observed at 1 and 2 wt. % GOx. The observed polymersome rupture results from the combination of two enzymatic reactions and transport of GOx and H_2O_2. Because transport phenomena and enzymatic reactions occur simultaneously, it is difficult to analyze the effect of each enzymatic reaction independently. However, since both the onset and termination decrease with increasing GOx concentration, obviously the kinetics of rupture can controlled by varying the enzyme (GOx) concentration. Furthermore, we can also tune the release rate of the encapsulated materials by altering the enzyme concentration because the slopes of the curves in Figure 2(c) increase with GOx concentration. Representative rupture video for each GOx concentration is provided in Supplementary Information.

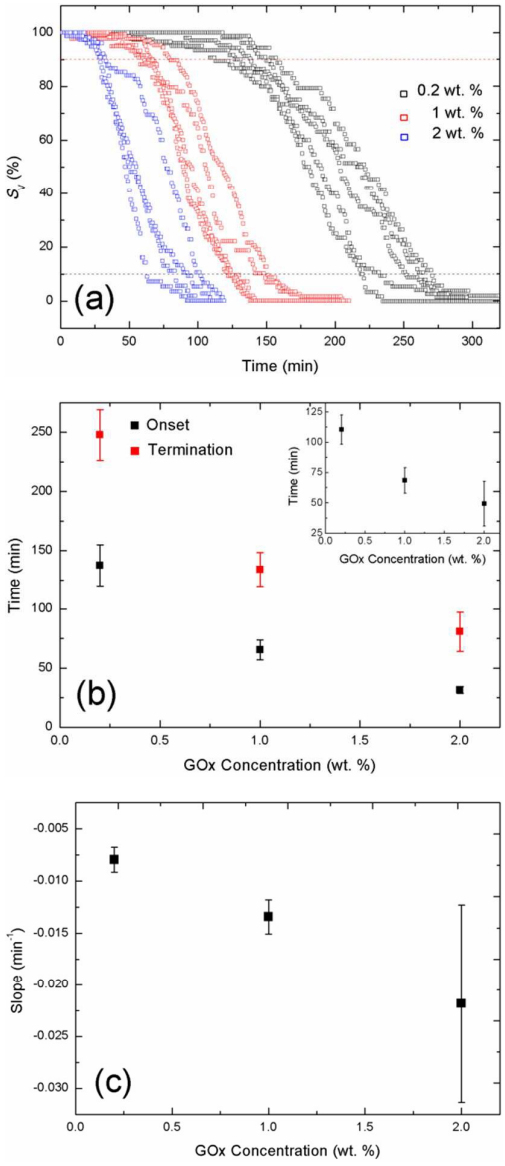

Figure 2. (a) The rupture of catalase-loaded polymersomes changes in GOx concentrations. (b) The onset and termination time for each

GOx concentration. Inset shows the active duration for each GOx concentrations. (c) The averaged slopes for each GOx concentration.

To confirm the effect of enzymatic reactions on polymersome rupture, we compared the S_V of polymersomes for a complete system with all the chemical components to that seen in distinct three control systems, each of which lacks at least one critical component. For GOx(–) control, the experiment was identical to the complete system except GOx was omitted. Based on GOx(–) control experiments, we could quantify naturally occurring polymersome rupture in the absence of the first enzymatic reaction. For catalase(–) control experiments, catalase-free polymersomes were dispersed in the D-glucose solution, followed by addition of GOx; that is, the second enzyme reaction was eliminated. This control tests whether the first enzymatic reaction itself can lead to the destabilization of polymersomes. For H_2O_2(–) control, we eliminated both enzymatic reactions. Catalase-free polymersomes were dispersed in the D-glucose solution and 0.2 ml of 2, 3, 5, 10, and 20 vol. % H_2O_2 were added in place of GOx solution. The resulting H_2O_2 concentration for the addition of 0.2 ml of 2, 3, 5, 10, and 20 vol. % H_2O_2 is 0.28, 0.43, 0.78, 1.43, and 2.86 vol. %, respectively. Supplementary Information provides the S_V for each concentration. From H_2O_2(–) control, we can confirm the stability of polymersome membrane in the presence of only H_2O_2, which is a known oxidizing agent. Figure 3(b) shows the S_V for the complete system, GOx(–), catalase(–), and H_2O_2(–) control. It took 288.0 ± 31.6 minutes to achieve complete rupture (S_V (t = 288 minutes) = 0) for the complete system. In contrast, the survivability S_V (t = 300 minutes) for GOx(–), catalase(–), and H_2O_2(–) controls were 98.3 ± 1.4, 96.3 ± 3.3, and 96.6 ± 3.8 %, respectively. These control experiments conclusively indicate that both enzymatic reactions are necessary to induce polymersome rupture.

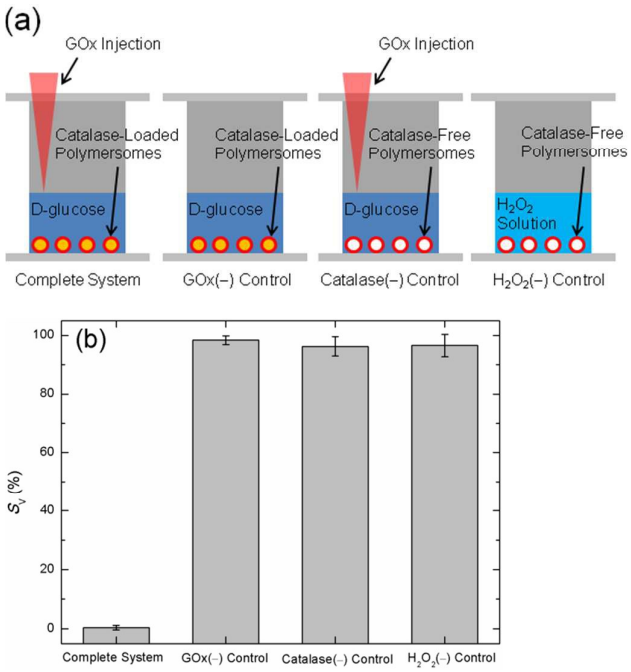

Figure 3. (a) Schematic illustration for the complete system and three control experiments. (b) S_V (t = 300 minutes) for complete system, GOx(–) control, catalase(–), and H_2O_2(–) controls. Results for complete system show the injection of 0.2 wt. % (0.0077 mM) GOx solution. Five different experiments were performed. In each experiment, initial number of polymersomes were 73.4 ± 19.2. For GOx(–), catalase(–), and H_2O_2(–) controls, three different experiments were performed. The initial number of polymersomes for GOx(–), catalase(–), and H_2O_2(–) controls were 37.3 ± 4.6, 75.3 ± 25.3, and 34.7 ± 6.1, respectively.

Although it is clear that both enzymatic reactions play a central role in the rupture of polymersomes, we interestingly did not observe the formation of gaseous bubbles in the vesicle lumen. We hypothesize that the consumption of O_2 in the first enzymatic reaction (See Figure 1(a) for the schematic of the D-glucose-GOx reaction) keeps O_2 concentration below saturation. Consequently, O_2 generated from the second enzymatic reaction (H_2O_2-catalase reaction) dissolves in the solution and immediately diffuses out of the polymersome. Therefore, the generation of gas bubbles and in turn an increase in the internal pressure of the polymersome is not likely the main cause of polymersome disruption, which leads to the question: what is the mechanism of rupture for catalase-encapsulated polymersomes?

Recent studies have shown that proteins can associate with bilayer membranes.[8, 35-41] Lipid membranes, for example, have been employed as model membranes for protein incorporation.[35, 36, 40] Hydrophobic sequences of proteins form pores on the membrane followed by the stabilization of membrane-protein hybrids. Furthermore, subsequent studies showed the stabilization of protein on polymer bilayer membranes.[37-39, 41] The high flexibility and conformational freedom of amphiphilic polymer chains lead to the stabilization of protein on polymer bilayer membrane.[39] Similarly, we hypothesized that catalase may directly associated with the membrane. From Figure 4b, catalase is locally concentrated at the edge of polymersome patch, which is topological defect between uniform membrane and thick polymersome patch. Thus, catalase can easily penetrate and be stabilized at the edge of polymersome patch. We assume that this association may play a role in membrane disruption. To verify the location of catalase in our assemblies, we encapsulated fluorescently labeled catalase in the polymersome lumen. Previously, other laboratories have shown that the use of microfluidic double emulsions led to the formation of patches on the outer surfaces of polymersomes.[26, 27, 42] After the evaporation the organic solvent mixture, the excess polymer remains on the polymersome membrane and forms a thick patch, as seen in Figure 4(a). Thus, both catalase-loaded and catalase-free polymersomes have patches on their membranes. Supplementary Information provides the optical and confocal micrographs of catalase-free polymersomes. Scanning laser confocal microscopy shows that catalase is both uniformly distributed within the lumen of polymersomes [as seen in Inset I of Figure 4(b)], and at the edge of the patches [as seen in the Inset II of Figure 4(b)]. These results suggest that the local concentration of catalase around the patches is high possibly due to the membrane association of catalase.

To verify whether catalase is associated with the polymersome membrane, we characterized the mechanical properties of catalase-loaded polymersomes using micropipette aspiration. Our previous study showed that the incorporation of surface active agents such as proteins leads to changes in the area modulus of polymersomes.[3] Micropipette aspiration applies suction on a microcapsule through a narrow glass capillary and correlates the areal strain (α) to the membrane tension (T_V), which is measured using a manometer: $\alpha = \alpha_0 + T_V/K_a$ where α_0 is a term representing thermal undulation of the membrane and K_a is the area expansion modulus.[42, 43] When the effect of thermal undulation on the

membrane behavior is released by initial tension, the relationship between T_V and α can be expressed as

$$T_V = K_a \cdot \alpha \qquad (1)$$

Figure 4(c) shows the aspiration results of catalase-loaded polymersomes. Membrane tension generated by micropipette suction resulted in a linear increase in areal strain and showed a reversible recovery upon decreasing membrane tension similar to our previous work.[3] However, Figure 5(d) shows that K_a for catalase-loaded polymersomes (K_a = 112.9 ± 5.8 dyne/cm) is statistically larger from that of catalase-free polymersomes (K_a = 97.2 ± 2.8 dyne/cm) indicating that the polymersomes membrane is tougher due to the presence of catalase. The results we present from confocal microscopy and micropipette aspiration strongly suggest that some amount of catalase is associated with the polymersome membrane.

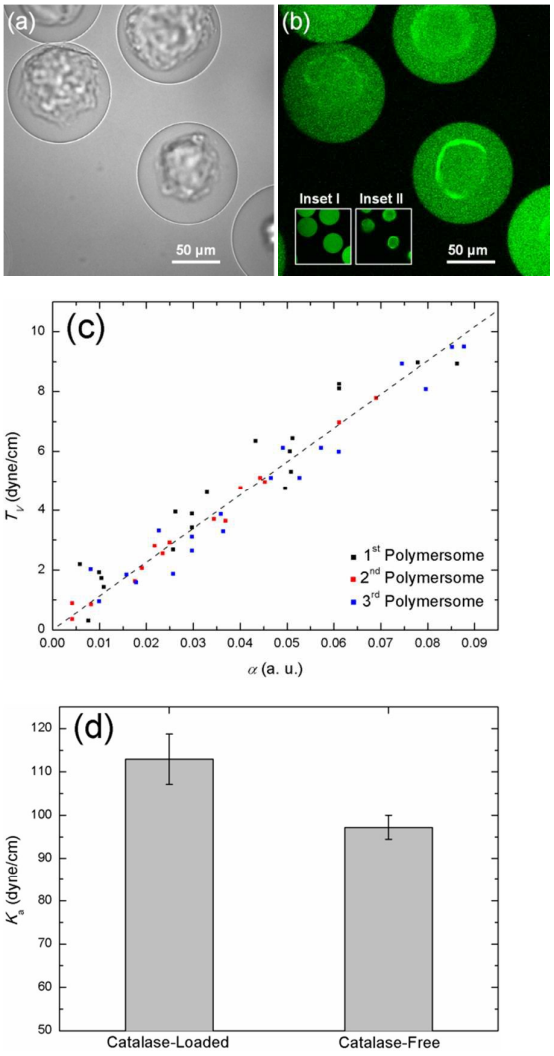

Figure 4. (a) Optical micrograph for catalase-loaded polymersomes. Bumpy and rough areas reflect the excessive polymer segregated into patches. (b) Stacked confocal micrograph for catalase-loaded polymersomes. Inset I and II show the confocal micrographs near the equator and patch, respectively. (c) The aspiration results of catalase-loaded polymersomes. Membrane tension generated by micropipette suction resulted in a linear increase in areal strain and showed a reversible recovery upon decreasing membrane tension. (d) K_a for catalase-loaded polymersomes (K_a = 112.9 ± 5.8 dyne/cm) is statistically different from that of catalase-free polymersomes (K_a = 97.2 ± 2.8 dyne/cm).

Based on these observations, we hypothesize that the direct interaction between H_2O_2 and membrane-associated catalase causes the rupture of polymersomes. Previous studies also have reported the rupture of polymersomes resulting from the interaction between membrane-associated substrate and free enzyme.[17, 18] Furthermore, membrane-associated photosystem II (PSII) enzyme shows high rates of enzymatic reaction.[45] This enzymatic reaction was ascribed to a membrane-associated heme catalase in PSII.[46, 47] Figure 5(a) shows the conceptual structure of polymersome membrane and associated catalase. To verify the direct interaction between H_2O_2 and adsorbed catalase in the polymersome membrane, we tested whether catalase can be associated into the polymersome membrane from outside after polymersome assembly. We dispersed catalase-free polymersomes in a 0.6 μg/ml catalase solution and aged the polymersomes for two weeks. The aged polymersomes were then dispersed in the D-glucose bath, followed by the addition of GOx. Figure 5(b) compares the S_V (t = 300 minutes) for the previously verified complete system to the S_V (t = 300 minutes) for catalase-free polymersomes that had been aged in catalase solutions for two weeks. Polymersomes not exposed to catalase are also shown (called zero-week aged). While zero-week aged polymersomes show a very high S_V, two-week aged polymersomes show significant disruption [S_V (t = 300 minutes) = 33.4 ± 21.3 %] as shown in Figure 5(b). These results strongly support our hypothesis that catalase, whether added to the lumen or outside of polymersomes, associates with the polymersome membrane and plays a crucial role in the disruption of polymersomes. Although we do not fully understand the detailed mechanism by which the membrane is disrupted by the membrane-associated catalase, our results strongly suggest that the interactions between H_2O_2 generated from the first enzymatic reaction and the membrane-associated catalase causes local defects in the membrane, which in turn lead to catastrophic rupture of polymersomes.

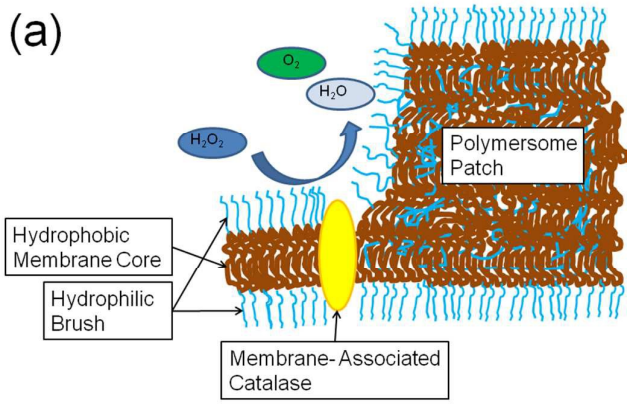

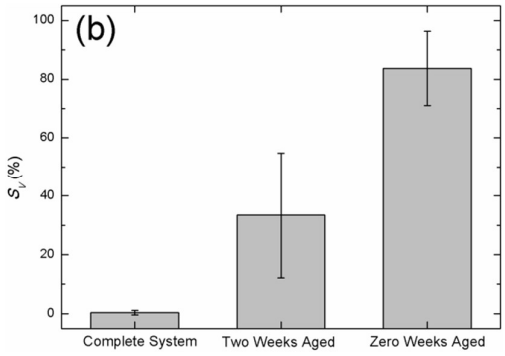

Figure 5. (a) Hypothetical structure for polymersome membrane and associated catalase. (b) S_V at 300 minutes for complete system, vesicles exposed for two weeks to catalase, and vesicles not exposed to catalase. Results were that S_v were 0.4 ± 0.8, 33.4 ± 21.3, and 83.7 ± 12.7 %, respectively.

Conclusions

In summary, we illustrate the triggered rupture of polymersomes controlled by two sequentially and geometrically arranged enzymatic reactions. First, we prepared catalase-loaded polymersomes using a microfluidic W/O/W double emulsion, which enables complete encapsulation of catalase. The catalase-loaded polymersomes were dispersed in the osmolality-matched D-glucose bath followed by GOx addition, which initiated the first enzymatic reaction. H_2O_2 generated from GOx reaction interacts with catalase-loaded polymersomes, leading to their rupture. This programmable rupture of polymersomes could be used to facilitate the precise release of active ingredients. Even though the polymersomes prepared by microfluidic double emulsion are rather large with diameter of 50–100 μm, the sequence of two enzymatic reactions we exploited in this work is a biologically relevant process. Thus, microfluidic double emulsion-templated polymersomes can serve as model systems to develop small polymersomes for in vivo applications.

Experimental

Polymersomes were prepared using poly(ethylene oxide-*b*-butadiene) (Polymer Source, Montreal, Canada). This polymer was synthesized by a standard living anionic polymerization technique.[48] Molecular weights for ethylene oxide and butadiene blocks are 1.3 and 2.5 kDa/mol, respectively. The polydispersity index of polymers is 1.05. We refer to this polymer as OB29. Chloroform, hexane, PBS, sucrose, bovine serum albumin (BSA), catalase, D-glucose, and GOx were purchased from Sigma Aldrich (St. Louis, MO). Fluorescently labeled catalase was purchased from NANOCS (Boston, MA). Fluorescein isothiocyanate (FITC) tagged with *N*-hydroxysuccinimide esters (NHS esters) react with primary amines in catalase.

W/O/W double emulsions were formed by a glass capillary microfluidic device as reported previously.[49] The aqueous inner and oil middle phases were focused by aqueous outer phase to generate W/O/W double emulsions. Details regarding device configuration and flow rates are provided in Supplementary Information. To prepare the inner phase, 40 mg of catalase was added to the 20 ml of 290 mOsm sucrose solution followed by vigorous stirring for one hour. The catalase-loaded sucrose solution was, then, filtered using a 0.22 μm-pore filter. To obtain fluorescent images, 1 mg of FITC-labeled catalase was added to the filtered solution. Osmolality for filtered solution was adjusted to 290 mOsm using 10X PBS and MilliQ water. The final catalase concentration for the inner phase was 0.60 ± 0.06 mg/ml. The middle phase had 2 mg/ml OB29 in the mixture of chloroform (38 vol. %) and hexanes (62 vol. %). The outer phase was 290 mOsm PBS. To increase the stability of double emulsions and polymersomes, 1 wt. % of BSA was added in the continuous phase.[50] Double emulsions were collected in a Petri dish containing 290 mOsm PBS. Collected double emulsions were stored at room temperature for 12 hours to evaporate the solvent. After 12 hours, formed polymersomes were gently transferred to a 20 ml vial and stored at 4°C for two weeks to ensure complete removal of the solvent. Polymersome rupture was observed using Zeiss Axiovert 200 (Oberkochen, Germany). Fluorescent and confocal micrographs were acquired by Nikon Eclipse TE300 (Chiyoda, Japan) and Olympus IX81 (Tokyo, Japan), respectively. The osmolalities of D-glucose solution and of the polymersome lumen were adjusted to 290 mOsm prior to each experiment. 0.2 ml of GOx solution was then gently injected into the experimental chamber. The polymersome rupture was observed using an inverted microscope. Protein concentrations were measured by Nanodrop ND-1000 Spectrophotometer (Wilmington, DE). Micropipette aspiration was performed by custom-made pipette and manometer. Details regarding pipette preparation and experimental procedures were explained elsewhere.[3]

Acknowledgements

This work was supported in its entirety by the Biomolecular Materials program at the U. S. Department of Energy, Office of Basic Energy Science, Division of Materials Science (DE-SC0007063). The authors also thank Dr. Miju Kim for helpful discussion regarding protein labeling.

References

1. H. Bermudez, A. K. Brannan, D. A. Hammer, F. S. Bates and D. E. Discher, *Macromolecules*, 2002, **35**, 8203-8208.
2. B. M. Discher, Y. Y. Won, D. S. Ege, J. C. M. Lee, F. S. Bates, D. E. Discher and D. A. Hammer, *Science*, 1999, **284**, 1143-1146.
3. W.-S. Jang, S. Park, M. Kim, J. Doh, D. Lee and D. A. Hammer, *Macromolecular Rapid Communications*, 2014.
4. N. P. Kamat, M. H. Lee, D. Lee and D. A. Hammer, *Soft Matter*, 2011, **7**, 9863-9866.
5. F. Meng, Z. Zhong and J. Feijen, *Biomacromolecules*, 2009, **10**, 197-209.
6. I. Louzao and J. C. M. van Hest, *Biomacromolecules*, 2013, **14**, 2364-2372.
7. R. J. R. W. Peters, M. Marguet, S. Marais, M. W. Fraaije, J. C. M. van Hest and S. Lecommandoux, *Angewandte Chemie-International Edition*, 2014, **53**, 146-150.
8. C. Martino, S.-H. Kim, L. Horsfall, A. Abbaspourrad, S. J. Rosser, J. Cooper and D. A. Weitz, *Angewandte Chemie-International Edition*, 2012, **51**, 6416-6420.
9. H. Lomas, I. Canton, S. MacNeil, J. Du, S. P. Armes, A. J. Ryan, A. L. Lewis and G. Battaglia, *Advanced Materials*, 2007, **19**, 4238-+.
10. F. Ahmed, R. I. Pakunlu, A. Brannan, F. Bates, T. Minko and D. E. Discher, *Journal of Controlled Release*, 2006, **116**, 150-158.
11. S. Li, B. Byrne, J. Welsh and A. F. Palmer, *Biotechnology Progress*, 2007, **23**, 278-285.

12. F. Ahmed and D. E. Discher, *Journal of Controlled Release*, 2004, **96**, 37-53.
13. H. Iatrou, H. Frielinghaus, S. Hanski, N. Ferderigos, J. Ruokolainen, O. Ikkala, D. Richter, J. Mays and N. Hadjichristidis, *Biomacromolecules*, 2007, **8**, 2173-2181.
14. P. S. Pramod, R. Shah, S. Chaphekar, N. Balasubramanian and M. Jayakannan, *Nanoscale*, 2014, **6**, 11841-11855.
15. N. A. Christian, M. C. Milone, S. S. Ranka, G. Li, P. R. Frail, K. P. Davis, F. S. Bates, M. J. Therien, P. P. Ghoroghchian, C. H. June and D. A. Hammer, *Bioconjugate Chemistry*, 2007, **18**, 31-40.
16. P. P. Ghoroghchian, J. J. Lin, A. K. Brannan, P. R. Frail, F. S. Bates, M. J. Therien and D. A. Hammer, *Soft Matter*, 2006, **2**, 973-980.
17. S. Haas, N. Hain, M. Raoufi, S. Handschuh-Wang, T. Wang, X. Jiang and H. Schoenherr, *Biomacromolecules*, 2015, **16**, 832-841.
18. K.-S. Tücking, V. Grützner, R. E. Unger and H. Schönherr, *Macromolecular Rapid Communications*, 2015, **36**, 1248-1254.
19. S. Nomura, K. Tsumoto, T. Hamada, K. Akiyoshi, Y. Nakatani and K. Yoshikawa, *Chembiochem*, 2003, **4**, 1172-1175.
20. D. Graefe, J. Gaitzsch, D. Appelhans and B. Voit, *Nanoscale*, 2014, **6**, 10752-10761.
21. W. Tai, R. Mo, J. Di, V. Subramanian, X. Gu, J. B. Buse and Z. Gu, *Biomacromolecules*, 2014, **15**, 3495-3502.
22. U. H. Yildiz, H.-P. M. De Hoog, Z. Fu, N. Tomczak, A. N. Parikh, M. Nallani and B. Liedberg, *Small*, 2014, **10**, 442-447.
23. A. Napoli, M. J. Boerakker, N. Tirelli, R. J. M. Nolte, N. Sommerdijk and J. A. Hubbell, *Langmuir*, 2004, **20**, 3487-3491.
24. Y. Elani, R. V. Law and O. Ces, *Nature Communications*, 2014, **5**.
25. N. P. Kamat, G. P. Robbins, J. Rawson, M. J. Therien, I. J. Dmochowski and D. A. Hammer, *Advanced Functional Materials*, 2010, **20**, 2588-2596.
26. H. C. Shum, J.-W. Kim and D. A. Weitz, *Journal of the American Chemical Society*, 2008, **130**, 9543-9549.
27. H. C. Shum, E. Santanach-Carreras, J.-W. Kim, A. Ehrlicher, J. Bibette and D. A. Weitz, *Journal of the American Chemical Society*, 2011, **133**, 4420-4426.
28. H. Lomas, J. Du, I. Canton, J. Madsen, N. Warren, S. P. Armes, A. L. Lewis and G. Battaglia, *Macromolecular Bioscience*, 2010, **10**, 513-530.
29. J. Z. Du, Y. Q. Tang, A. L. Lewis and S. P. Armes, *Journal of the American Chemical Society*, 2005, **127**, 17982-17983.
30. P. P. Ghoroghchian, P. R. Frail, K. Susumu, D. Blessington, A. K. Brannan, F. S. Bates, B. Chance, D. A. Hammer and M. J. Therien, *Proceedings of the National Academy of Sciences of the United States of America*, 2005, **102**, 2922-2927.
31. P. J. Photos, L. Bacakova, B. Discher, F. S. Bates and D. E. Discher, *Journal of Controlled Release*, 2003, **90**, 323-334.
32. L. Tretter and V. Adam-Vizi, *Journal of Neuroscience*, 2004, **24**, 7771-7778.
33. A. A. Starkov, in *Mitochondria and Oxidative Stress in Neurodegenerative Disorders*, eds. G. E. Gibson, R. R. Ratan and M. F. Beal, 2008, vol. 1147, pp. 37-52.
34. M. Forkink, J. A. M. Smeitink, R. Brock, P. H. G. M. Willems and W. J. H. Koopman, *Biochimica Et Biophysica Acta-Bioenergetics*, 2010, **1797**, 1034-1044.
35. K. Bauer, A. Schmid, W. Boos, R. Benz and J. Tommassen, *European Journal of Biochemistry*, 1988, **174**, 199-205.
36. R. Benz and K. Bauer, *European Journal of Biochemistry*, 1988, **176**, 1-19.
37. D. Ho, B. Chu, H. Lee and C. D. Montemagno, *Nanotechnology*, 2004, **15**, 1084-1094.
38. D. Ho, B. Chu, J. J. Schmidt, E. K. Brooks and C. D. Montemagno, *Ieee Transactions on Nanotechnology*, 2004, **3**, 256-263.
39. W. Meier, C. Nardin and M. Winterhalter, *Angewandte Chemie-International Edition*, 2000, **39**, 4599-+.
40. M. Winterhalter, *Colloids and Surfaces a-Physicochemical and Engineering Aspects*, 1999, **149**, 547-551.
41. D. Wong, T.-J. Jeon and J. Schmidt, *Nanotechnology*, 2006, **17**, 3710-3717.
42. H. C. Shum, D. Lee, I. Yoon, T. Kodger and D. A. Weitz, *Langmuir*, 2008, **24**, 7651-7653.
43. E. Evans and W. Rawicz, *Physical Review Letters*, 1990, **64**, 2094-2097.
44. W. Rawicz, K. C. Olbrich, T. McIntosh, D. Needham and E. Evans, *Biophysical Journal*, 2000, **79**, 328-339.
45. Y. G. Sheptovitsky and G. W. Brudvig, *Biochemistry*, 1996, **35**, 16255-16263.
46. W. D. Frasch and R. Mei, *Biochemistry*, 1987, **26**, 7321-7325.
47. W. D. Frasch and R. Mei, *Biochimica Et Biophysica Acta*, 1987, **891**, 8-14.
48. M. A. Hillmyer and F. S. Bates, *Macromolecules*, 1996, **29**, 6994-7002.
49. R. K. Shah, H. C. Shum, A. C. Rowat, D. Lee, J. J. Agresti, A. S. Utada, L.-Y. Chu, J.-W. Kim, A. Fernandez-Nieves, C. J. Martinez and D. A. Weitz, *Materials Today*, 2008, **11**, 18-27.
50. N. P. Kamat, S. J. Henry, D. Lee and D. A. Hammer, *Small*, 2013, **9**, 2272-2276.